IEEE Access
Multidisciplinary ⋮ Rapid Review ⋮ Open Access Journal

Received August 17, 2021, accepted September 7, 2021, date of publication September 10, 2021,
date of current version September 20, 2021.

Digital Object Identifier 10.1109/ACCESS.2021.3111927

Data-Driven Methods for Battery SOH Estimation: Survey and a Critical Analysis

TSUYOSHI OJI[1], YANGLIN ZHOU[2], (Student Member, IEEE), SONG CI[2], (Senior Member, IEEE), FEIYU KANG[3], XI CHEN[4], AND XIULAN LIU[4], (Member, IEEE)

[1]Tsinghua-Berkeley Shenzhen Institute, Tsinghua University, Shenzhen 519071, China
[2]Department of Electrical Engineering, Tsinghua University, Beijing 100084, China
[3]Shenzhen Key Laboratory for Graphene-Based Materials, Engineering Laboratory for Functionalized Carbon Materials, Tsinghua Shenzhen International Graduate School, Tsinghua University, Shenzhen 518055, China
[4]Beijing Electric Power Research Institute, Beijing 100075, China

Corresponding author: Song Ci (sci@tsinghua.edu.cn)

This work was supported in part by the Regional Key Research and Development Program of Inner Mongolia Autonomous Region in China under Grant 2020ZD0018, and in part by the Science and Technology Foundation of State Grid Corporation of Beijing under Grant 52022319005Q.

ABSTRACT State-of-health (SOH) estimation is a critical factor in ensuring the efficiency, reliability, and safety of lithium-ion batteries (LIBs) in electric vehicles (EVs). However, due to the complexity of electrochemical processes in batteries and the dynamics of working conditions, it is challenging to estimate SOH accurately, especially in real-world EV application scenarios. Thus, various data-driven methods with robust and adaptive features for SOH estimation have been widely proposed in the current literature. However, there is a lack of a comprehensive investigation and performance comparison of those methods, which makes them hard to be adopted in practice. Hence, in this paper, we have studied current major data-driven methods with real-world EV battery data to evaluate the performance. Besides, we summarize each method's advantages and limitations with the consideration of the critical features required to achieve accurate SOH estimation in real-world applications. Hopefully, this paper provides a practical insight into the related fields.

INDEX TERMS Lithium-ion battery, state of health, data-driven methods, state estimation.

I. INTRODUCTION

With the merit of a long lifetime, high energy density, and fast response, lithium-ion batteries (LIBs) are widely used in electric vehicles (EVs) and energy storage scenarios [1], [2]. However, LIB performance declines over time (calendar aging) and use (cycle aging), which can lead to degraded performance, operational impairment, or even catastrophic consequences [3]. Since the complex internal electrochemical properties and uncertain external working environments, LIB degradation is an extremely complex process (as shown in Fig. 1), including physical mechanisms (e.g., thermal stress and mechanical stress) and chemical mechanisms (e.g., side reactions) [4], [5]. Generally, state of health (SOH) estimation is a critical metric in a battery management system (BMS) to quantify the extent of degradation. The most frequently used SOH indicator is battery capacity, which is defined as the ratio of current maximum available capacity C_i over the nominal value C_0 as $SOH = \frac{C_i}{C_0} \times 100\%$. With the gradually aging, when SOH reaches $70\% - 80\%$, LIBs are more prone to thermal runaway and cause a safety risk [6]. An accurate and robust SOH estimation method ensures the safety, reliability, and cost-efficiency of a battery during operation [7].

In general, the methods for SOH estimation methods can be categorized into direct estimation and data-driven methods. Direct estimation usually includes Coulomb Counting and Impedance Spectroscopy [8]. In Coulomb counting, the integral of current is calculated with respect to time and divide by their difference of state of charge (SOC). It is a simple and widely used method, but its results are rather inaccurate, and the errors would accumulate [9]. Impedance spectroscopy applies a wide frequency spectrum to determine SOH [10]. However, the impedance spectroscopy method needs to carry out numerous experiments and requires adequate intermediate time to rest before the cell reaches its balanced potential.

Even though data-driven models have been applied in numerous SOH estimation processes, few available

The associate editor coordinating the review of this manuscript and approving it for publication was Giambattista Gruosso.

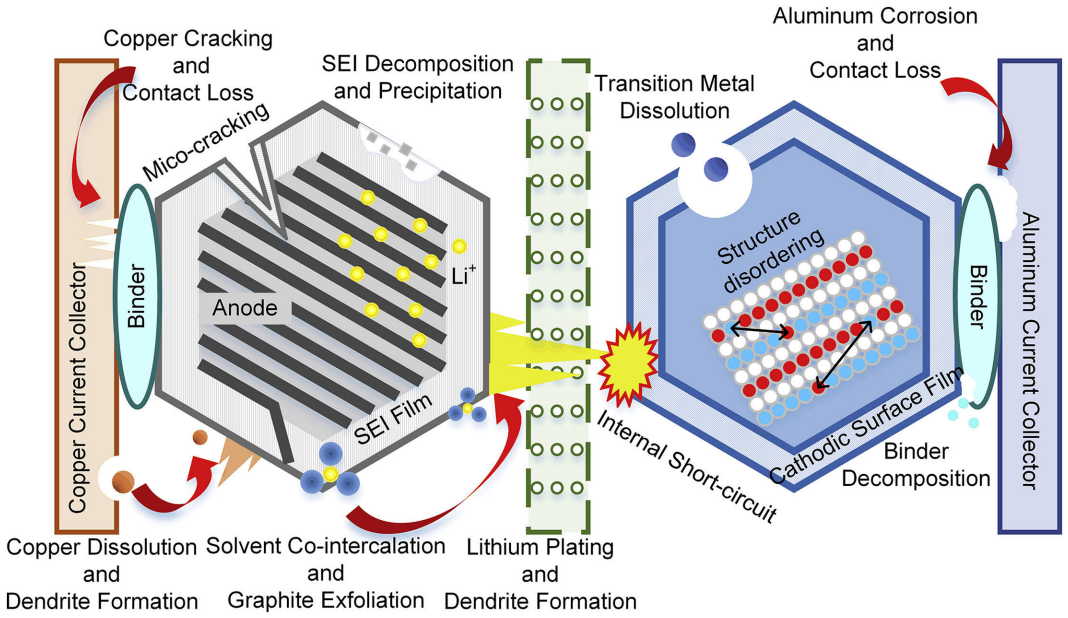

FIGURE 1. Degradation mechanisms in Li-ion cells.

investigations were focusing on the comprehension performance of each method. Andre *et al.* only compared the estimation performances of Neural Network (NN) and Extended Kalman Filter (EKF) for their accuracy and training speed [11]. Saha *et al.* employed Autoregressive Integrated Moving Average (ARIMA), EKF, Particle Filter (PF), and Relevance Vector Machine (RVM) to estimate the remaining useful life (RUL) for LIBs [12]. Each method's algorithm is specifically introduced, but the estimation performance results were only presented in figures without a quantitative comparison. In [8], [13]–[16], various data-driven methods were studied for their pros and cons, and the methods were classified into different categories but lacking an objective performance comparison.

To address the aforementioned challenges, this paper makes the following main contributions:

- Review the major data-driven SOH estimation approaches for LIBs reported in the recent literature.
- Compare the performance of three model-based models and four model-less models, namely EKF, PF, ARIMA, Extreme Learning Machine (ELM), Long Short-term Memory (LSTM), Support Vector Machine (SVM), and RVM, on a real-world EV dataset.
- Provide an overall discussion about the aforementioned models in terms of their accuracies, confidence intervals, abilities to deal with nonlinearity, robustness, computation complexities, capabilities to deal with data sparsity, and generalization.

The remainder of this paper is organized as follows: For different data-driven methods, Section II provides a short theoretical explanation, their challenges, and a literature review focused on SOH estimation application. In Section III, the real-world operation EV data are shown, and the comparison experiment of previously described methods is explained in detail. The comparison result is analyzed and discussed in Section IV. In Section V, the different models previously described are discussed for actual application requirements. Section VI presents the conclusion drawn from this paper. For the reader' convenience, Tab1 lists all the acronyms used in this article in alphabetical order.

II. REVIEW OF DATA-DRIVEN ESTIMATION METHODS

The data-driven approach is a method that builds a rough model and then refines the model with numerous data to make the model consistent with the data. If the initial model is an existing battery model, it is classified as a model-based method; otherwise, it is a model-less method.

The existing battery model in model-based methods usually involves Equivalent Circuit Model (ECM) and electrochemical model. ECM model uses appropriate circuit components to constitute an equivalent circuit, and the parameters of the circuit model can only obtain under laboratory conditions and will change through battery aging. The electrochemical model is to study the electrochemical process through battery aging, and its strength resides on no laboratory measurement required. However, developing a detailed mathematical model including phase-changing typically requires cell disassembly [17].

On the other hand, model-less methods can avoid analyzing the complex electrochemical reaction and directly use machine learning approaches to estimate the aging process. Such methods do not need prior knowledge of battery type and working conditions. The accuracy of the estimation largely depends on the training data size. Nevertheless, in most machine learning methods, we need to select a set of external characteristics that can best represent SOH, which may bring subjective factors into the estimation process.

TABLE 1. List of acronyms and abbreviations.

Acronym	Description	Acronym	Description
ACF	Autocorrelation Function	MCMC	Markov Chain Monte Carlo
ANN	Artificial Neural Network	MLP	Multi-layer Perceptron
AR	Autoregressive	MSE	Mean Square Error
ARD	Automatic Correlation Determination	NN	Neural Network
ARIMA	Autoregressive Integrated Moving Average	BMS	Battery Management System
PACF	Partial Autocorrelation Function	CALCE	Center for Advanced Life Cycle Engineering
PCC	Possibilistic Clustering Classification	CNN	Convolutional Neural Network
PCoE	Prognostics Center of Excellence	CPSO	Continuous Particle Swarm Optimization
PDF	probability density function	DCNN	Deep Convolutional Neural Network
PF	Particle Filter	DPSO	Discrete Particle Swarm Optimization
PSO	Particle Swarm Optimization	EAPs	Electrode Aging Parameters
RBF	Radial Basis Function	ECM	Equivalent Circuit Model
RMSE	Root Mean Square Error	EKF	Extended Kalman Filter
RMSProp	Root Mean Square Prop	ELM	Extreme Learning Machine
RNN	Recurrent Neural Netwokr	EVs	Electric Vehicles
RUL	Remaining Useful Life	FFNN	Feed Forward Neural Network
RVM	Relevance Vector Machine	GBR	Gradient Boosted Regression
SampEn	Sample Entropy	GPR	Gaussian Process Regression
SLFN	Single Hidden Layer Feed Forward Neural Networks	HI	Health Indicator
SMC	Sequential Monte Carlo	KF	Kalman Filter
SOC	State of Charge	LIB	Lithium-ion Battery
SOH	State of Health	LSTM	Long Short-term Memory
SVM	Support Vector Machine	MAE	Mean Absolute Error
SVR	Support Vector Regression	MAPE	Mean Absolute Percentage Error
UKF	Unscented Kalman Filtering	MC	Monte Carlo
UPF	Unscented Particle Filter		

TABLE 2. Different capacity degradation models.

No.1	Selected model
1	$C = a \times k^2 + b \times k + c$
2	$C = a \times exp(b \times k) + c \times k + d$
3	$C = a \times exp(b \times k) + c \times k^2 + d$
4	$C = a \times exp(b \times k) + c \times k^2 + d \times k + e$
5	$C = a \times exp(b \times k) + c \times exp(d \times k)$
6	$C = \frac{a \times C_1}{b \times C_1 + (a - b \times C_1) \times exp(a \times k)}$

a, b, c, d and e are the parameters in those models; k is the number of cycles; C_1 in No.6 is a constant through empirical test;

A. MODEL-BASED METHODS

As mentioned earlier, model-based methods usually contain an ECM or electrochemical model. ECM model is mainly used to confirm SOC and difficult to estimate the remaining capacity. Hence, the electrochemical model is adopted to estimate SOH. Table 2 shows different electrochemical models for SOH estimation [18].

The model parameters can be determined through adaptive filter methods. The main concept is to filter the measurement noise so it can update the model parameters with new measurements. Kalman Filter (KF) and PF are two common methods adopted for this purpose.

1) KALMAN FILTER (KF)

KF is a statistical-based filtering method proposed in 1960. Through repeated iterations of the previous estimate and the current measurement values, a relatively accurate value can be derived. The state equation in KF is used to describe the state process of the system based on the prior information, and the measurement value obtained by the external observation system is described by using the measurement equation [19].

However, the standard KF cannot solve the nonlinear degradation model, so there are some improved algorithms such as EKF and Unscented Kalman Filtering (UKF).

The basic principle of EKF is to use the expansion of the Taylor series to linearize the nonlinear equation and then to solve the linearized equation using the KF framework. Therefore, it may be more suitable for battery state estimation. Plett *et al.* showed that although EKF was usually used in SOC estimation in the past decades, it may also be used to estimate power fade and can keep the SOC estimate accurate throughout the cell lifetime even though its dynamics changing as it ages [20]. Before using the differential quotient to calculate the state matrix and the measurement matrix, Zhou *et al.* combined Gaussian Process Regression (GPR) with EKF to approximate the state equation, the measurement equation, and the noise equation of EKF [21].

In addition, UKF [22] was proposed in estimation process at [23] and [24]. The advantage of UFK is that there is no specific form of the nonlinear equation, so there is no demand for the derivative and Jacobian matrix calculation.

2) PARTICLE FILTER (PF)

In PF, the particles are generated and recursively updated from a nonlinear process that involves a system under analysis, a measurement model, and a priori estimate of the state probability density function (PDF) [25]. That is to say, using Monte Carlo (MC) simulations, PF is a method for implementing a recursive Bayesian filter, and this is also known as the Sequential MC (SMC) method.

With regard to PF-based methods, Su *et al.* divided the model into three categories: polynomial model, exponential model, and Verhulst [26] model, to compare their

performance [18]. Miao *et al.* presented an improved PF algorithm, the unscented particle filter (UPF), which combined the idea of PF and UKF to improve the RUL prediction accuracy [27]. UPF can be divided into two steps: firstly, the UKF method was used to get the proposal distribution; secondly, the standard PF method was applied to get the final results. Zhang *et al.* proposed an improved UPF based on the Markov chain Monte Carlo (MCMC) method, in which, after resampling in UPF, MCMC was adopted to approximate the estimated state [28]. Therefore, it can maintain the particle's diversity and suppress particle degradation to a certain extent. Some other work also tried to solve the importance function chosen and degradation of diversity in sampling particles problems, using the linear optimization approach to produce new particles from chosen particles and abandoned particles [29].

3) AUTOREGRESSIVE INTEGRATED MOVING AVERAGE (ARIMA)

ARIMA requires only the historical time series data. This model is fitted to time series data to forecast future points in the series. Therefore, ARIMA is more suitable for single-step estimation instead of multi-step prediction.

In an ARIMA model, the choice of its parameters is usually subjective. In this regard, Long *et al.* used a high-order Autoregressive (AR) model to replace the ARIMA model and transformed the problem of seeking nonlinear parameters of ARIMA into seeking linear parameters in the AR model [30]. Furthermore, he proposed the Particle Swarm Optimization (PSO) algorithm to avoid the uncertainty of human subjective order determination. The data metabolic technology is also used to make the AR model change adaptively.

In order to improve the accuracy in the long-term prediction process, Liu *et al.* introduced an influence factor to characterize 'accelerated' degradation and combined this influencing factor with the AR model [31]. In his following work [32], he introduced a regularized particle filter to further improve the prediction accuracy.

B. MODEL-LESS METHODS

Instead of considering the electrochemical reaction and the failure mechanism inside batteries, the model-less methods, which require no explicit battery models and regard the battery system as a black box, and then infer battery SOH or lifespan directly from extracted features. In literature, many statistical, computational, and artificial intelligence algorithms and models, such as Artificial Neural Network (ANN) [33]–[38], SVM [39], [40], RVM [41], [42], GPR [43], Gradient Boosted Regression (GBR) [44], [45], have been adopted for battery state estimation in various applications. However, data-driven techniques are usually unstable as they may show different performances with different datasets [46]. Among all these model-less methods, ANNs and SVMs are regarded as the two most representative ones for nonlinear modeling [47].

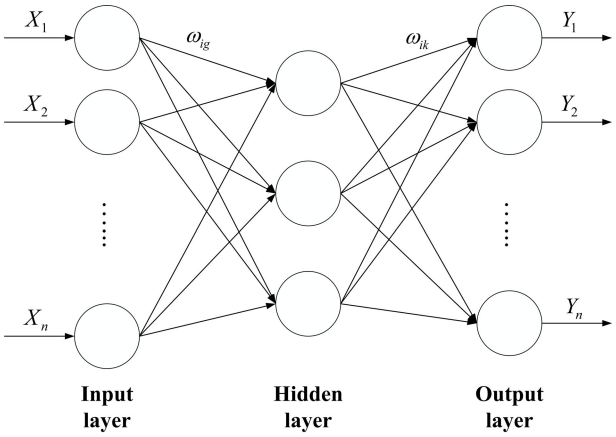

FIGURE 2. A topological structure of BP neural network.

1) ARTIFICIAL NEURAL NETWORK (ANN)

ANN is intended to imitate the human brain's behavior, with artificial neurons arranged at the input layer, hidden layer(s), and output layer, respectively. The ANN topology is illustrated in Fig. 2. The input layer gathers the preprocessed information and acts as a conduit to the hidden layer(s). Each neuron can be represented by a weighted linear combination and contains a mathematical model based on its input for determining its output in the hidden layers [48]. The ANN-based method has long been used for modeling as they provide automated knowledge extraction and high inference accuracy if a sufficient amount of operation data is used for model training [49]. There are many kinds of network selection methods. A typical type having been successfully applied for SOH estimation is Feed Forward Neural Network (FFNN), also known as Multi-layer Perceptron (MLP), which is usually trained by the back-propagation algorithm.

So far, it is generally believed that the internal resistance is the most representative feature of the remaining useful capacity of the battery. Xia *et al.* used FFNN to prove the relationship between the complex impedance zero-phase crossing frequency of a battery and its SOH [33]. However, the measurement speed of internal resistance is usually slow, which is almost impossible to realize for online applications. Zhang *et al.* proposed an online method for SOH and RUL monitoring based on the fusion of partial incremental capacity and FFNN [34]. After smoothed the initial partial incremental curve and carried out the Spearman correlation analysis, two strongly correlated features were extracted from the partial incremental curve as input, and then two FFNN models for simultaneous estimation of SOH and RUL were established, leading to a simple model structure and the satisfactory accuracy and generalization performance.

However, ANNs usually suffer from slow training speed and high computational requirements. Therefore, a kind of fast learning model called ELM has been proposed for onboard estimation.

2) EXTREME LEARNING MACHINE (ELM)

Different from other ANNs, the connection weight between the input layer and hidden layer and the threshold of the hidden layer can be set randomly, with no adjustment required after setting. Moreover, the connection weights between the hidden layer and the output layer can not be adjusted iteratively but determined by solving the generalized inverse matrix [50]. Thus, compared with the traditional neural networks, especially with the Single Hidden Layer Feed Forward Neural Network (SLFN), it delivers faster performance than traditional learning algorithms in the premise of ensuring learning accuracy.

Pan *et al.* used the Thevenin equivalent model to calculate the ohmic internal resistance and polarization internal resistance of the battery with easily measured terminal voltage, load current, and ambient temperature [35]. The increment of the two resistance values was taken as the health factor, and the ELM method was used to estimate the battery life online. Compared with the traditional FFNN, the results showed that the estimation error is significantly reduced with a faster training speed.

3) DEEP LEARNING NETWORK

With multi-layer perceptron and hidden layers, the concept of deep learning is originated from the ANN and rising in recent years. Shen *et al.* first applied the deep learning method to the online capacity estimation of Li-ion batteries [36]. He utilized a deep convolutional neural network (DCNN) for the battery capacity estimation based on the voltage, current, and charge capacity measurements during a partial charge cycle. The proposed structure successfully avoids the manual feature extraction process, which has the risk of dropping useful information. Tian *et al.* also construct a convolutional neural network (CNN) to estimate electrode capacities and initial SOCs, termed electrode aging parameters (EAPs) [51].

Recurrent Neural Network (RNN) is another type of the deep learning methods that have certain advantages in learning nonlinear features of sequences. With the assumption that the attenuation of battery capacity is continuous in time, Eddahech *et al.* demonstrated an RNN model to predict the remaining capacity and internal resistance through the collected SOC difference, pulse current, temperature, and three latest-predicted internal resistance values [37].

However, RNN suffers from learning long-term dependencies. If RNN stores information over a period of time, the network gradient tends to vanish, meaning that the network is unable to learn anymore. Zhang *et al.* synthesized a data-driven battery RUL predictor by using Long Short-term Memory Recurrent Neural Network (LSTM-RNN) [38]. The Root Mean Square Prop (RMSProp) method for small batch training data samples was used to train the constructed neural network [52], and a rejection technique was proposed to solve the over-fitting problem [53]. The results showed that with similar accuracy, compared with other methods [18], [54]–[57], the number of offline training data samples can be reduced by 20% - 50%.

4) SUPPORT VECTOR MACHINE (SVM)

The main concept of SVM is to find a small set of support vectors out of a large number of data samples, which can still describe the system. SVM has been successful in a wide range of applications, especially for nonlinear problems with small samples, and can effectively prevent local minimization. In theory, there is a global optimum and can avoid the defect of the local extremum. Nevertheless, it is sometimes troublesome to determine the optimal kernel function and hyperparameters for nonlinear modeling [47].

In [39], PSO was employed to obtain the Support Vector Regression (SVR) kernel parameter. By adopting a fresh validation method, the fusion PSO–SVR model can well grasp the global degradation trend of SOH with little interference from local regenerations and fluctuations. Tao *et al.* imbedded the PF method into the SVR paradigm to optimize the hyperparameters due to its ability to update the parameters dynamically, providing the PDF of the optimal parameters [40]. Possibilistic Clustering Classification (PCC) was also induced to cluster different operational states to clusters and then estimate through their belonging model.

Another drawback of SVM is lacking the ability to output the confidence intervals, so the variation model, RVM, is widely adopted.

5) RELEVANCE VECTOR MACHINE (RVM)

RVM is also a supervised learning method similar to SVM. It is based on the Bayesian framework theory, which can eliminate the irrelevant points through the Automatic Correlation Determination (ARD) and then derive the sparse model. Compared with SVM, RVM can construct any kernel function without the restriction of the Macy's theorem. In terms of parameters, SVM needs to be initialized manually, and different values may have a great influence on the results, while RVM can be operated automatically.

However, RVM involves a combination of kernel functions, and determining the weight of each function is vital to the performance. In [58], Yang *et al.* proposed a fusion method by using the Discrete Particle Swarm Optimization (DPSO) [59] algorithm for selecting kernels adaptively, and Continuous Particle Swarm Optimization (CPSO) [60] to adjust kernel combinations as well as kernel parameters adaptively.

In order to find an alternative online health indicator (HI) to quantify the battery degradation, Zhou *et al.* chose the mean voltage falloff as a HI in each charging and discharging cycle [42]. After the extraction, Box-Cox transformation was adopted to enhance the degree of linear correlation between the HI and the capacity. Then the author compared the performance of the simple statistical regression model and the RVM model. The result indicated that the proposed RVM model was more accurate than the simple statistical regression model and with the confidence interval.

To verify the SVM and RVM performance, Widodo *et al.* used the Sample Entropy (SampEn) [61] as a HI to estimate

TABLE 3. A synopsis of the reviewing results for the data-driven estimation methods.

Method	Reference	Description of experiment dataset	Estimation precision	Novelty
KF	[20]	7.5 Ah & 5 Ah $LiMn_2O_4$/Graphite	the estimation converge to the correct values	Using dual and joint EKF to estimate power fade and capacity fade
	[21]	Battery pack on electric bus	Error <8%	Proposed an iterated GPR-EKF algorithm for online in-use EV SOH estimation
	[24]	18650-type lithium battery	Error <0.1%	Designed a Double Unscented KF to calculate SOC and SOH at the same time
PF	[18]	A1, A2, A3, and A4 from CALCE[a]	accurate estimation	Proposed an interacting multiple model particle filter for estimating the RUL with an improved battery capacity degradation model
	[27]	A1, A2, A3, and A4 from CALCE	Error <5%	Introducing the unscented particle filter into the battery RUL prediction
	[28]	A1, A2, A3, and A4 from CALCE	Error 2.04%	Proposed an improved unscented particle filter for LIB RUL prediction based on Markov chain Monte Carlo
	[29]	#5, #6, #7, and #18 from PCoE[b]	Error $\leq$ 4.6%	Using linear optimizing combination resampling to improve the prediction accuracy of the unscented particle filter
ARIMA	[30]	A1, A2, A3, and A4 from CALCE	Error <14.6%	Using particle swarm optimization to improve the AR model
	[31]	#5, #6, #7, and #18 from PCoE and CS2-8, CS2-21, and CS2-33 from CALCE	MAE[c] <10% in most of the cases	Introducing an optimized nonlinear degradation AR time series model for RUL estimation
ANN	[33]	Tenergy 30005-0 LIB	N/A	Presenting a SOH estimation method based on the complex impedance zero-phase crossing frequency of a battery
	[34]	#5, #6, #7, and #18 from PCoE	MAE in range of 2.79-3.52	Proposed a novel on-line synthesis method based on the fusion of partial incremental capacity and ANN to estimate SOH and RUL
ELM	[35]	ICR 1850-26F from Samsung, $LiNMC$/Graphite	Maximum Error 2.22%, MAE 1.72%	Introducing an ELM to capture the underlying correlation between the internal resistance and capacity degradation to improve the speed and accuracy for SOH estimation
CNN	[36]	20 cells from PCoE and 10-years cycling tests on eight Li-ion cells	Maximum Error <9.479%	Utilizing DCNN for battery capacity estimation based on the voltage, current, and charge capacity measurements during a partial charge cycle
	[51]	eight Kokam pouch $Li(NiCoAl)O_2$/Graphite	Error <1.6%	Using CNN to estimate electrode capacities and initial SOCs
RNN	[37]	$LiN_xCo_yAL_zO_2$/Graphite	MSE[d] 0.462	Using RNN to monitor the SOH
LSTM	[38]	NCR 18650PF from Panasonic, $Li(NiCoAl)O_2$/Carbon	Error <11.6%	Using LSTM and RNN to predict the RUL, and a dropout technique is adopted to address the overfitting problem
SVM	[39]	#5, #6, #7, and #45 from PCoE	MAPE[e] 0.82%-2.28%	Using particle swarm optimization to obtain the SVR kernel parameter for SOH estimation
	[40]	one Li-ion battery from PCoE	accurate estimate	Using the possibilistic clustering classification to determine the system, particle filtering to select SVR parameters according to the system state, and predicate remaining useful cycle through SVR
RVM	[41]	#18 and #28 from PCoE	RMSE[f] 0.54	Using SampEn as a HI to estimate SOH by using RVM
	[42]	#5 from PCoE	RMSE 0.0135	Choosing the mean voltage falloff as a HI in each charging and discharging cycle, and estimating the capacity through RVM model

[a]Batteries data from NASA Ames Prognostics Center of Excellence. [b]Batteries data from the Center for Advanced Life Cycle Engineering at the University of Maryland. [c]Mean Absolute Error. [d]Mean Square Error. [e]Mean Absolute Percentage Error. [f]Root Mean Square Error.

SOH through both methods [41]. The results showed that RVM outperforms SVM-based battery health prognostics in the aspect of accuracy.

So far, the primary data-driven estimation methods in the literature have been reviewed, and a detailed synopsis of the estimation results is provided in Table 3. As can be seen from the table, the dataset is vital to the estimation performance. Most of these studies used the publicly available data from NASA Ames Prognostics Center of Excellence (PCoE) [62], or the Center for Advanced Life Cycle Engineering (CALCE) at the University of Maryland [56]. However, even with the same dataset, some articles proposed abnormally highly accurate estimation results, which may bring confusion to actual implementation. Therefore, it is necessary to evaluate the performance of major data-driven methods on a real-world dataset with the same evaluation indices.

III. A COMPREHENSIVE AND QUANTITATIVE STUDY WITH REAL-WORLD DATA

As mentioned earlier, different types of models exhibit controversial results since they had been tested with different data sets. Therefore, in this work, we have chosen the aforementioned major data-driven methods for battery SOH estimation

FIGURE 3. The electric bus studied in this work.

TABLE 4. Specifications of the electric bus and the battery pack.

Item	Specification
the total number of buses	6
location	Yingshang County, Fuyang City, Anhui Province, China
vehicle model	LCK6809EVGM1
motor model	TZ405XSD11
total weight	11700 kg
maximum speed	69 km/h
rated/peak power	80/135 kw
nominal voltage	560 V
battery type	IFP20100140A
operation time	Jan.2017 - Jun.2019
data sampling interval	30 s
data attributes	total voltage, total current, and other 20 features
operation temperature	-5 to 50°C
total data volume	~1 million data records

based on real-world operation EV data and compare their performance.

A. REAL-WORLD BATTERY OPERATION DATA

The real-world data adopted in this work was obtained from six electric buses running in Yingshang County, Fuyang City, Anhui Province in China. An electric bus is shown in Fig. 3. All buses are loaded with lithium iron phosphate battery packs produced by Hefei Gotion High-tech Power Energy CO., Ltd.

BMS units are used for logging all battery operate data, including voltage, current, temperature, and 20 other parameter values. The data logging interval is 30 seconds, and the time frame of the recorded data is from January 2017 to June 2019. The specifications of the electric bus and the battery pack data are summarized in Table 4.

Due to the dynamics of discharging process, which makes it difficult to calculate the remaining useful capacity during the discharging process. However, the charging current remains at a relatively stabilized value. Hence, the charge capacity of a battery pack can be expressed as:

$$Q_i = \int_{t_{i2}}^{t_{i1}} Idt \tag{1}$$

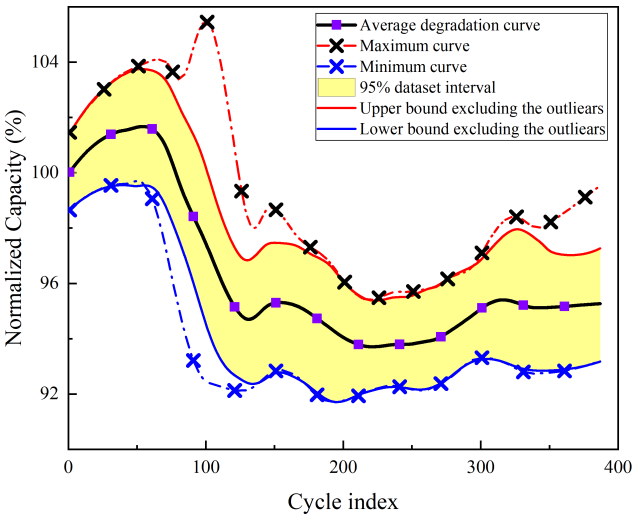

FIGURE 4. Diagram of six set of capacity degradation curve.

where Q_i stands the total capacity charged in i cycle. t_{i1} and t_{i2} represents the initial charging time and ending time, respectively. Accordingly, the available capacity of the battery pack was:

$$C_i = \frac{Q_i}{SOC_{end} - SOC_{star}} \times 100. \tag{2}$$

As shown in (2), the denominator will approach zero when the difference of SOC is small. Hence, we only consider the deep charging cycle (SOC difference $\geq 30\%$).

As we mentioned in Section I, since SOH quantifies the degradation degree of LIBs, it will provide guidance for battery replacement [63]. Most current research works use characterization parameters of battery aging (e.g., capacity, internal resistance, and power) to define SOH [64]. Among those parameters, internal resistance can only be acquired in the laboratory condition, and power measurement makes the computation more complex. Hence, for convenience in real-world applications and maximum efficiency, SOH in this paper is defined as the ratio of current maximum available capacity C_i over the nominal value C_0, as:

$$SOH = \frac{C_i}{C_0} \times 100\% \tag{3}$$

In this study, four hundred deep charging cycles were selected for each bus. After ranking the absolute percentage error between each data point and the average value in the corresponding cycle, the data points with the highest five percentage errors were regarded as outliers. Their curve diagrams and the statistical results are shown in Fig. 4 and Table 5, respectively. It can be seen that some onboard measurement data points show large deviations, and the calculated remaining useful capacity dropped about 8% at around the hundredth cycle for all six datasets. Therefore, an appropriate data-driven estimation model must be able to reject those outliers.

TABLE 5. The statistics results derived from six curves.

Criteria	Value
average standard deviation	2.03%
average range	5.38%
average memory size	23.14KB

B. EXPERIMENTAL SETTINGS

For the data-driven methods mentioned above, some data-driven models can not deal with the time series directly, so it's necessary to use other features to train them. In addition, the optimization algorithms can not automatically optimize some parameters called hyperparameters, which need to be set manually. Therefore, the following is a description of the selected features and hyperparameters of the models used in this paper. These hyperparameters are determined through cross-validation, but there is no guarantee that all parameters are the globally optimal values.

1) EXTENDED KALMAN FILTER

By using the No.6 capacity degradation model listed in the Table 1 as the measurement equation and the four parameters adding noise as the estimation equation, EKF iterates through the Kalman gain and updates four parameters of the model when new measurement data are available. The four parameters and covariance matrix are initialized to '[0.5, 0, 0.5, 0]' and '[1; 0.005; 1; 0.005]', respectively. We have also adopted the one-step estimation method, i.e., estimating the next cycle SOH from the existing model, because the radical change SOH in real-world applications may not be estimated by a fixed model and then need to be updated in a real-time fashion.

2) PARTICLE FILTER

The PF model is developed with the same measurement equation and initial parameters as used in EKF. One-step estimation is adopted as same as used in EKF.

3) AUTOREGRESSIVE INTEGRATED MOVING AVERAGE

The ARIMA model is possible to handle the non-stationary series of data if the series of data can achieve stationary by differentiating it to a sufficient degree. Therefore, the parameters of the ARIMA model, including the differentiating times, 'd', autoregressive terms, 'p', and moving average terms, 'q', can be determined through the autocorrelation function (ACF) and the partial autocorrelation function (PACF). In our case, the model derives the best estimation performance when (p, d, q) is set to '4,1,2'.

4) EXTREME LEARNING MACHINE

Different from the model-based algorithms, model-less methods estimate SOH through observing a few external feature values. In this paper, five values - starting SOC, ending SOC, starting voltage, ending voltage, and average charging current - extracted from the battery charging data sets are used to train the ELM model. In our case, we set the activation function as the hyperbolic tangent activation function and a single hidden layer with 30 nodes.

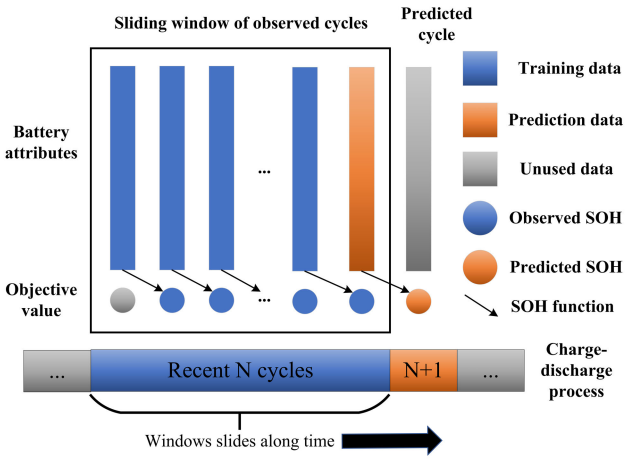

FIGURE 5. Prediction procedure with a sliding window of N in the recent observation cycles: The relationship between attributes in the current cycle and the SOH in the next cycle is modeled by the attributes of first N cycles, which are used as the training data; the SOH in the future is forecasted by the attributes of the last/current cycle, which are used as the prediction data; the rest of cycles beyond the sliding window are irrelevant to the prediction of SOH in this cycle.

5) SUPPORT VECTOR MACHINE

For the SVM model, the five values mentioned above in ELM are used to train this model, the penalty coefficient is 100, and the kernel function is radial basis function (RBF) with a variance of 16.67.

6) RELEVANCE VECTOR MACHINE

For the RVM model, the aforementioned five values in ELM are also used to train the RVM model, and the kernel function is RBF.

7) LONG SHORT-TERM MEMORY

LSTM cannot directly process the time series, so the time series obtained by a sliding window is used to train the LSTM model. As shown in Fig. 5, previous N−1 cycles are used to form the observation matrix, with the SOH of the subsequent cycles as the target value [65]. In our case, the size of the sliding window is ten, and the neuron in the single hidden layer is four.

The experiments are conducted on a computing platform with Intel Core i7-6700K processor at 4.0 GHz using 32 GB of RAM, running Win10 Pro version.

IV. PERFORMANCE EVALUATION AND ANALYSIS

To compare the performance of the aforementioned data-driven models, 10% of one dataset preprocessed as described in Section III-A are used for training, and the remaining 90% are used for testing. The corresponding estimation results are shown in Fig. 6(a). It can be seen that the SOH estimation results for EKF, PF, and LSTM models are closer to the real SOH than ARIMA, ELM, SVM, and RVM model results.

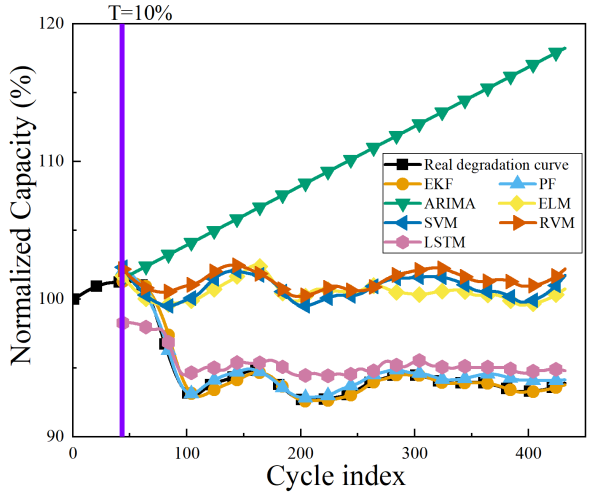

(a) The performance of SOH estimation for seven different models with 10% data samples for training.

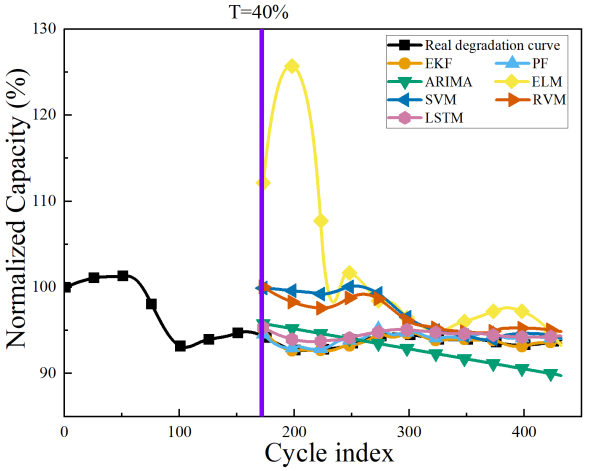

(b) The performance of SOH estimation for seven different models with 40% data samples for training.

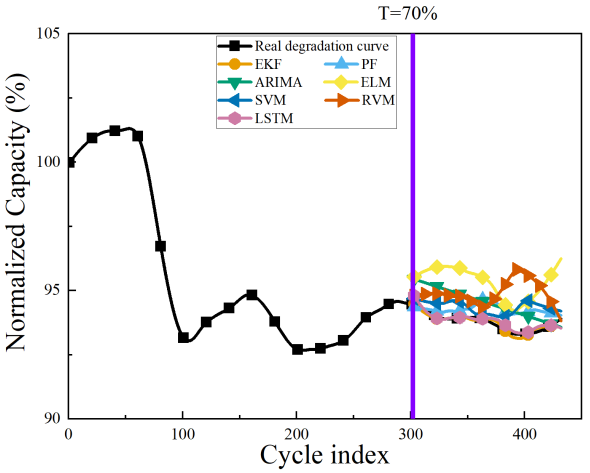

(c) The performance of SOH estimation for seven different models with 70% data samples for training.

FIGURE 6. **Real and predicted SOH using size of training set.**

The fitting curve for ARIMA even shows an upward trend in the rest of the life cycle, indicating a large estimation error contained within. The error mainly comes from the outliers from the training data because ARIMA is not equipped with any mechanism to reject those outliers. After training, the intrinsic structure was fixed, and the estimation results were only related to the cycle index.

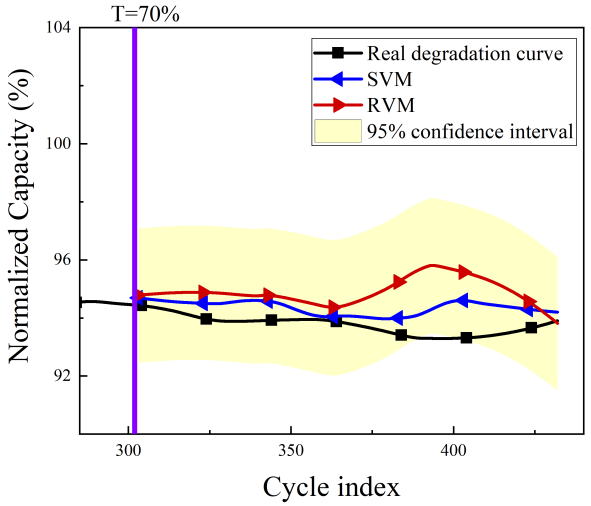

FIGURE 7. **The performance of SOH estimation for SVM and RVM models with 70% data samples for training.**

The estimation results for all the models mentioned above by using 40% data samples for training and 60% data samples for testing are shown in Fig. 6(b). It can be found that the results of EKF, PF, and LSTM methods are still closer to the real SOH than others. Specifically, the fitting curve for ELM shows a large deviation in the beginning, which is similar to what ARIMA presents by using 10% data samples for training. However, ELM failed to estimate SOH because it could not deal with data sparsity. The single hidden layer and the non-iterative training process in ELM would lead to underfitting with small training samples.

The estimation results for all aforementioned data-driven models by using 70% data samples for training and 30% data samples for testing are shown in Fig. 6(c). As is observed from the figure, the estimation results are all close to the real SOH, which validates the effectiveness of all the aforementioned models with the substantial number of training data samples. In this sense, confidence intervals for the outputs are more significant than their accuracy. The estimation results of RVM and SVM by using 70% data samples for training are compared with the real values and presented in Fig. 7. RVM is advantageous because it can output confidence intervals, and most of the real values reside in the 95% confidence interval of estimation results.

To further discuss the impacts of different size of training set on SOH estimation performance, we apply three metrics to evaluate the aforementioned models. The first metric is the mean absolute percentage error (MAPE) to evaluate the general accuracy, which are defined as follows:

$$MAPE = \frac{1}{m}\sum_{i=1}^{m}\left|\frac{y_i - \hat{y}_i}{\hat{y}_i} \times 100\%\right| \tag{4}$$

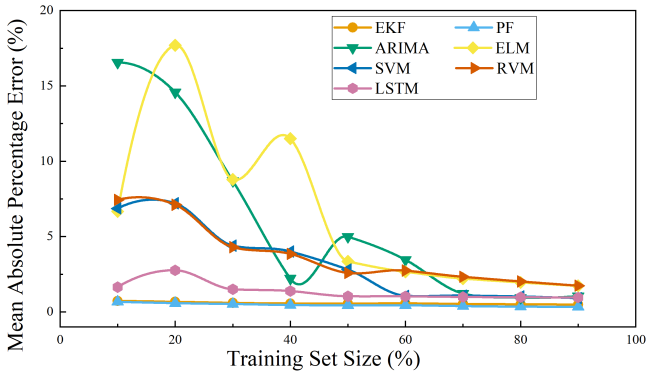

(a) The performance of MAPE influenced by different size of training set for seven different models.

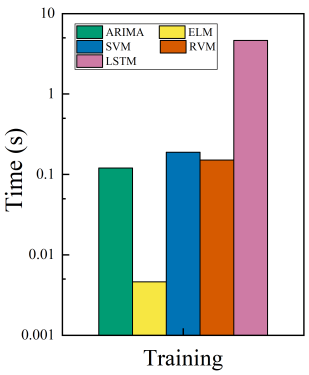

(b) The performance of average training time for five different models.

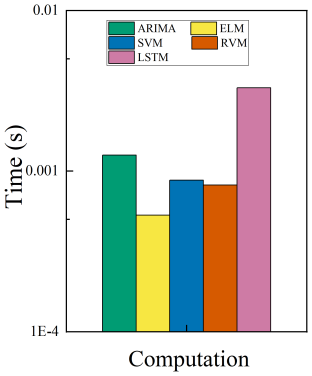

(c) The performance of average computation time for five different models.

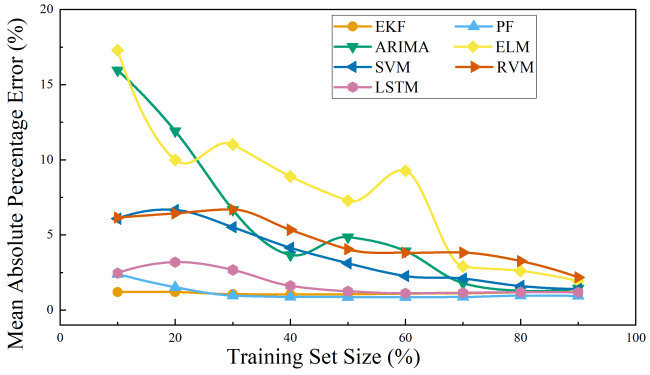

(d) The performance of average MAPE influenced by different size of training set for seven different models by using six different datasets.

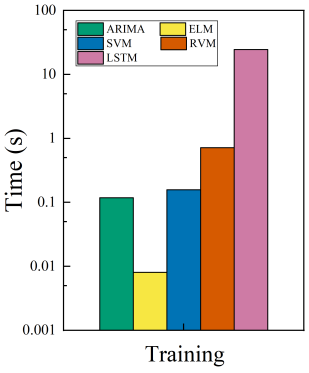

(e) The performance of average training time for five different models by using six different datasets.

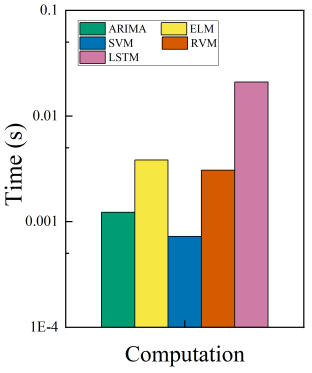

(f) The performance of average computation time for five different models by using six different datasets.

FIGURE 8. **The performance of SOH estimation influenced by different size of training set.**

where m is the total number of data samples; y_i and $\hat{y}_i$ are the estimated and real values of cycles i, respectively. The second metric is the time to train each model, and the third metric is the computational time to complete SOH estimation. The comparison of three metrics under different training set for each model by using one dataset are presented in Fig. 8(a), Fig. 8(b), and Fig. 8(c), respectively.

In Fig. 8(a), the MAPE of PF and EKF are lower than other methods across all sizes of training samples, while LSTM presented a similar accuracy after 50% of the data samples are used for training. The MAPE of ELM and ARIMA are over 7.5% before adopting 30% of data samples for training, indicating that both methods need substantial training samples to avoid underfitting. In addition, SVM outperforms RVM after using 60% data samples for training.

Fig. 8(b) and Fig. 8(c) show the average training and computation time of different models with varied training samples, respectively. The training and computation steps were interlaced in EKF and PF models so that the time results are not shown in Fig. 8(b) and Fig. 8(c). Among other data-driven models, the training speed of ELM is the fastest. For the rest of the models, the training speed of ARIMA is almost equal to that of SVM or RVM, whereas the LSTM model is more than ten times slower than others. However, although the computation times between LSTM and other methods are still vastly different by ten times, the absolute difference is only within 0.005s, which is tolerable in actual practice.

To find out a more generalized conclusion, the average MAPE, training time, and computation time results by using all the six datasets are shown in Fig. 8(d), Fig. 8(e), and Fig. 8(f), respectively. Each dataset is tested ten times and records to find the average result so as to reduce randomness to the utmost extent. The results are graphically depicted in Table 6. It can be seen that PF shows the best average accuracy, followed by EKF, LSTM, SVM, RVM, ARIMA, and ELM. However, ELM is the fastest model for training on average, followed successively by ARIMA, SVM, RVM, and LSTM. Additionally, the average computation speed of SVM is the fastest, followed by ARIMA, RVM, ELM, and LSTM. These rankings are similar as reported.

The above comparison results indicate that EKF and PF exhibit a relatively high accuracy (MAPE <2.5%) by using any proportion of data samples for training. In another word, as long as an electrochemical model and its initial parameters are correctly chosen, these adaptive filters could accurately estimate SOH without extensive operating data. However,

TABLE 6. The average estimation performance comparison of seven data-driven models by using different proportion of data samples from six different datasets for training.

Method	MAPE of different size of training set									Training time (s)	Computation time (s)
	10%	20%	30%	40%	50%	60%	70%	80%	90%		
EKF	1.19364	1.19732	1.05601	1.04395	1.05272	1.0892	1.10972	1.18162	1.2022	/	/
PF	2.39963	1.51994	0.95831	0.876	0.86599	0.86068	0.86946	0.96291	0.93727	/	/
ARIMA	15.95127	11.91511	6.67631	3.66746	4.85552	3.92903	1.78622	1.28315	1.44076	0.11826	0.00122
ELM	17.2826	10.00144	11.01737	8.89512	7.27004	9.27325	2.89588	2.60505	1.93132	0.00804	0.00384
SVM	6.08293	6.65947	5.51218	4.1482	3.11184	2.26234	2.09836	1.5942	1.39533	0.15769	7.24E-04
RVM	6.15237	6.43643	6.69633	5.33651	4.0446	3.81621	3.82658	3.25879	2.17791	0.71786	0.00308
LSTM	2.45766	3.18927	2.6711	1.61702	1.25421	1.11488	1.14831	1.19163	1.17996	24.5945	0.02098

this conclusion can only stand if high-precision data measurement devices are applied. Another model-based method, ARIMA, is somewhat on the opposite. Unlike EKF and PF, it needs a substantial set of data to fit with a time series model, which makes it more suitable for short-term prediction.

On the other hand, without requirements on prior knowledge, the 'black box' framework adopted in model-less methods would produce results that are entirely dependent on the training samples. Among these models, ELM is the fastest in training speed because no iteration was involved in its training. However, it suffers from low accuracy and the incapability to reject the outliers. On the opposite, LSTM demonstrates the best accuracy with the longest training time. SVM is superior to RVM in terms of accuracy, as well as shorter training and computation time. Despite that, RVM can output confidence intervals, which makes it one of the most prospective models in the future.

V. FURTHER DISCUSSION

Application categories and resource limits are determined in which cases a data-driven method can be applied. Thus, different elements should be viewed when choosing the appropriate method for a certain context [66]. In this section, some aspects that need considerations in future applications of LIB aging estimation will be discussed.

A. ACCURACY

The accuracy of a data-driven method is one way to indicate how successfully it fulfills its goal by a fair metric. For instance, EKF proposed in section IV was evaluated by MAPE, which was shown to be less than 3%. In this case, we can say it is a highly accurate method.

B. CONFIDENCE INTERVAL

When applying data-driven methods, the bias-variance tradeoff needs to be considered [67]. Those methods that specialize in error minimization are possible to end up with the overfitting issue. Therefore, instead of getting rid of errors, a better result should give a confidence interval within which the true value is located. In this regard, an ideal estimation model should be probabilistic so that it can provide a range of values to represent the estimation results with a specified confidence level.

Among all the methods reviewed, RVM employs a probabilistic Bayesian framework, while PF is based on Bayesian filtering and Monte Carlo simulation. Thus, both methods are capable of producing confidence intervals as their output.

C. ABILITY TO DEAL WITH NONLINEARITY

SOH recession is a strongly nonlinear process, so the capability to model nonlinear relations is crucial for data-driven methods. Both EKF and PF can take nonlinear equations for measurement and transition. Besides, ANN and SVM frameworks also allow nonlinear regressions. However, ARIMA is one of the linear regression models. Consequently, limitations could be seen in practical applications.

D. ROBUSTNESS

A severe limitation for current data-driven methods is that their development has been limited to aspects about measurement accuracy. In the literature, such measurement data were considered as known and accurate [68]. Nevertheless, when estimations are performed in practice, such data typically contain a certain amount of noise. This inaccurate measurement can lead to a huge estimation error, resulting in misleading conclusions. Hence, it is of practical importance to build a robust model against noises.

SVM and RVM involve robust mechanisms to deal with small data fluctuation and aberration. In fact, they are engaged with an inherent sparse mechanism that allows them to neglect small data variation, and RVM can even discard irrelevant data [68]. Besides, EKF is also competent in terms of noise exclusion. On the other hand, ARIMA and ELM do not include any comparable mechanism to reinforce estimation robustness. Furthermore, in PF, the outliers will also cause filter divergence, leading to unwanted estimation performance [25].

E. COMPUTATION COMPLEXITY

The computation complexity is evaluated as the resources required by a data-driven method to run. In particular, it focuses on their time (amount of time it takes to run an algorithm) and memory (amount of memory space required to solve an instance) requirements. The determination of a model's computational complexity is useful because by this way, we can (i) decide whether a part of the assignments should be carried out online or offline, (ii) distribute storage

TABLE 7. The summary of different models.

Methods		Model-based			Model-less			
		EKF	PF	ARIMA	ELM	SVM	RVM	LSTM
accuracy		high	high	low	low	medium	medium	high
confidence interval		×	✓	×	×	×	✓	×
ability to deal with nonlinearites		✓	✓	×	✓	✓	✓	✓
robustness		high	low	low	low	high	high	medium
capability to deal with data sparsity		high	high	low	low	medium	medium	medium
computation complexity	big-$\mathcal{O}$ time complexity	$\mathcal{O}(n)$	$\mathcal{O}(N_p)$	—[b]	Variable[c]	$\mathcal{O}(n^3)$	$\mathcal{O}(n^3)$	Variable[c]
	big-$\mathcal{O}$ memory complexity	$\mathcal{O}(1)$	Variable[a]	—[b]	Variable[c]	$\mathcal{O}(n^2)$	$\mathcal{O}(n^2)$	Variable[c]
generalization		low	low	low	medium	high	high	high

[a]Depending on the number of particles. [b]Big-$\mathcal{O}$ complexity cannot be defined [c]Depending on the input dimension, the number of training samples, the number of hidden units, and the number of outputs.

space in a more effective manner, and (iii) suggest modifications that would improve the computation results [66].

Since the computation complexity is generally difficult to quantify, one common representation of it is the asymptotic behavior expressed by big-$\mathcal{O}$ notations, which characterize functions according to the correlation between run time or space requirements and the input size in a data-driven method.

Among the aforementioned models, the complexity of PF is independent of the state dimension and increases by the function of the particle number (N_p). The corresponding time complexity is $\mathcal{O}(N_p)$ [68]. The computational complexity of ARIMA was found to depend on its order. In this sense, its big-$\mathcal{O}$ complexity cannot be determined. The computational complexity of the ANN framework model is varied based on the number of training samples, input dimensions, hidden units, and outputs [69].

F. CAPABILITY TO DEAL WITH DATA SPARSITY

Data sparsity is a term used to describe insufficient data in a dataset [70]. This is a common problem in data-driven methods since datasets for training are usually incomplete in many real-world applications. On the other hand, the computation time may grow to be unacceptable when the training data size exhibits a small increment because of the big-$\mathcal{O}$ complexity. Consequently, an ideal estimation model should achieve a high degree of accuracy with fewer training data, such as EKF and PF.

G. GENERALIZATION

In practice, thousands of single batteries are connected in series to form a package, making it inefficient to build the estimation models for each individual battery. Therefore, a generalized estimation model is essential, and such a model must react to a new dataset or a new battery without much training.

Model-based methods are based on a specific battery model (e.g., an electrochemical model) to estimate the battery SOH. Nevertheless, even batteries of the same prototype could exhibit completely different electrochemical models due to the variances in running conditions. On the other hand, model-less methods are more flexible because they are not subjective to such limitations.

The characteristics of the aforementioned SOH estimation methods are summarized in Table 7.

VI. CONCLUSION

Recently, data-driven approaches have been widely adopted to develop methods for accurate SOH estimation to ensure the efficiency, reliability, and safety of LIBs in EVs. Although data-driven methods have been applied in numerous SOH estimation processes, few comprehensive studies have compared the performance of these methods. Therefore, in this study, several different data-driven methods, namely EKF, PF, ARIMA, ELM, SVM, RVM, and LSTM, were investigated and evaluated. To our best knowledge, this is the first work to compare their performance with the real-world EV operation data.

The comparison showed that PF yielded the highest performance in terms of the average accuracy, while ELM was the model with the fastest training and SVM was the model with the fastest computation. Hence, none of the aforementioned methods can be considered an absolutely superior method, and a trade-off among the desired accuracy, the output confidence interval, the ability to deal with nonlinearity, robustness, computation costs, the ability to deal with data sparsity, and generalization should be considered for each particular situation. Table 7 gives a summary of the aforementioned methods.

Finally, this investigation is limited because only the different methods were compared, but the electrochemical model and HI might also affect the estimation performance. In the future, more explorations are needed by comparing the estimation inputs to provide insights into designs.

REFERENCES

[1] N. Nitta, F. Wu, J. T. Lee, and G. Yushin, "Li-ion battery materials: Present and future," *Mater. Today*, vol. 18, no. 5, pp. 252–264, 2015.
[2] R. Thomas, G. Despesse, S. Bacquet, E. Fernandez, Y. Lopez, P. Ramahefa-Andry, and L. Cassarino, "A high frequency self-reconfigurable battery for arbitrary waveform generation," *World Electr. Vehicle J.*, vol. 12, no. 1, p. 8, Jan. 2021.
[3] B. Gou, Y. Xu, and X. Feng, "State-of-health estimation and remaining-useful-life prediction for lithium-ion battery using a hybrid data-driven method," *IEEE Trans. Veh. Technol.*, vol. 69, no. 10, pp. 10854–10867, Oct. 2020.
[4] X. Hu, L. Xu, X. Lin, and M. Pecht, "Battery lifetime prognostics," *Joule*, vol. 4, no. 2, pp. 310–346, Feb. 2020.
[5] C. R. Birkl, M. R. Roberts, E. McTurk, P. G. Bruce, and D. A. Howey, "Degradation diagnostics for lithium ion cells," *J. Power Sources*, vol. 341, pp. 373–386, Feb. 2017.

[6] T. Duong, "USABC and PNGV test procedures [U.S. Advanced battery consortium (USABC); partnership for a new generation of vehicles (PNGV)]," *J. Power Sources*, vol. 89, pp. 244–248, Oct. 2000.
[7] H. Dai, G. Zhao, M. Lin, J. Wu, and G. Zheng, "A novel estimation method for the state of health of lithium-ion battery using prior knowledge-based neural network and Markov chain," *IEEE Trans. Ind. Electron.*, vol. 66, no. 10, pp. 7706–7716, Oct. 2019.
[8] M. H. Lipu, M. Hannan, A. Hussain, M. Hoque, P. J. Ker, M. Saad, and A. Ayob, "A review of state of health and remaining useful life estimation methods for lithium-ion battery in electric vehicles: Challenges and recommendations," *J. Cleaner Prod.*, vol. 205, pp. 115–133, Dec. 2018.
[9] K. S. Ng, C.-S. Moo, Y.-P. Chen, and Y.-C. Hsieh, "Enhanced Coulomb counting method for estimating state-of-charge and state-of-health of lithium-ion batteries," *Appl. Energy*, vol. 86, no. 9, pp. 1506–1511, Sep. 2009.
[10] K. B. Hatzell, A. Sharma, and H. K. Fathy, "A survey of long-term health modeling, estimation, and control of lithium-ion batteries: Challenges and opportunities," in *Proc. Amer. Control Conf. (ACC)*, Jun. 2012, pp. 584–591.
[11] D. Andre, A. Nuhic, T. Soczka-Guth, and D. U. Sauer, "Comparative study of a structured neural network and an extended Kalman filter for state of health determination of lithium-ion batteries in hybrid electricvehicles," *Eng. Appl. Artif. Intell.*, vol. 26, no. 3, pp. 951–961, Mar. 2013.
[12] B. Saha, K. Goebel, and J. Christophersen, "Comparison of prognostic algorithms for estimating remaining useful life of batteries," *Trans. Inst. Meas. Control*, vol. 31, nos. 3–4, pp. 293–308, 2009.
[13] W. Waag, C. Fleischer, and D. U. Sauer, "Critical review of the methods for monitoring of lithium-ion batteries in electric and hybrid vehicles," *J. Power Sources*, vol. 258, pp. 321–339, Jul. 2014.
[14] T. Wang, C. Zhu, L. Pei, R. Lu, and B. Xu, "The state of arts and development trend of SOH estimation for lithium-ion batteries," in *Proc. IEEE Vehicle Power Propuls. Conf. (VPPC)*, Oct. 2013, pp. 1–6.
[15] L. Unguream, G. Cârstoiu, M. V. Micea, and V. Groza, "Battery state of health estimation: A structured review of models, methods and commercial devices," *Int. J. Energy Res.*, vol. 41, no. 2, pp. 151–181, 2017.
[16] S. B. Sarmah, P. Kalita, A. Garg, X.-D. Niu, X.-W. Zhang, X. Peng, and D. Bhattacharjee, "A review of state of health estimation of energy storage systems: Challenges and possible solutions for futuristic applications of Li-ion battery packs in electric vehicles," *J. Electrochem. Energy Convers. Storage*, vol. 16, no. 4, Nov. 2019, Art. no. 040801.
[17] Q. Badey, G. Cherouvrier, Y. Reynier, J. Duffault, and S. Franger, "Ageing forecast of lithium-ion batteries for electric and hybrid vehicles," *Current Top. Electrochem.*, vol. 16, pp. 65–79, Jan. 2011.
[18] X. H. Su, S. Wang, M. Pecht, L. L. Zhao, and Z. Ye, "Interacting multiple model particle filter for prognostics of lithium-ion batteries," *Microelectron. Rel.*, vol. 70, pp. 59–69, Mar. 2017.
[19] Y. Kim and H. Bang, "Introduction to Kalman filter and its applications," in *Introduction and Implementations of the Kalman Filter*. London, U.K.: IntechOpen, 2018.
[20] G. L. Plett, "Dual and joint EKF for simultaneous SOC and SOH estimation," in *Proc. 21st Electr. Vehicle Symp.*, 2005, pp. 1–12.
[21] D. Zhou, P. Fu, H. Yin, W. Xie, and S. Feng, "A study of online state-of-health estimation method for in-use electric vehicles based on charge data," *IEICE Trans. Inf. Syst.*, vol. 102, no. 7, pp. 1302–1309, 2019.
[22] S. J. Julier and J. K. Uhlmann, "New extension of the Kalman filter to nonlinear systems," *Proc. SPIE*, vol. 3068, pp. 182–193, Apr. 1997.
[23] Y. Cai, Q. Wang, and W. Qi, "D-UKF based state of health estimation for 18650 type lithium battery," in *Proc. IEEE Int. Conf. Mechatronics Automat.*, Aug. 2016, pp. 754–758.
[24] Q. Wang, Y. Jiang, and Y. Lu, "State of health estimation for lithium-ion battery based on D-UKF," *Int. J. Hybrid Inf. Technol.*, vol. 8, no. 7, pp. 55–70, Jul. 2015.
[25] Z. Chen, "Bayesian filtering: From Kalman filters to particle filters, and beyond," *Statistics*, vol. 182, no. 1, pp. 1–69, 2003.
[26] W. Xian, B. Long, M. Li, and H. Wang, "Prognostics of lithium-ion batteries based on the Verhulst model, particle swarm optimization and particle filter," *IEEE Trans. Instrum. Meas.*, vol. 63, no. 1, pp. 2–17, Jan. 2014.
[27] Q. Miao, L. Xie, H. Cui, W. Liang, and M. Pecht, "Remaining useful life prediction of lithium-ion battery with unscented particle filter technique," *Microelectron. Rel.*, vol. 53, no. 6, pp. 805–810, Jun. 2013.
[28] X. Zhang, Q. Miao, and Z. Liu, "Remaining useful life prediction of lithium-ion battery using an improved UPF method based on MCMC," *Microelectron. Rel.*, vol. 75, pp. 288–295, Aug. 2017.
[29] H. Zhang, Q. Miao, X. Zhang, and Z. Liu, "An improved unscented particle filter approach for lithium-ion battery remaining useful life prediction," *Microelectron. Rel.*, vol. 81, pp. 288–298, Feb. 2018.
[30] B. Long, W. Xian, L. Jiang, and Z. Liu, "An improved autoregressive model by particle swarm optimization for prognostics of lithium-ion batteries," *Microelectron. Rel.*, vol. 53, no. 6, pp. 821–831, 2013.
[31] D. Liu, Y. Luo, Y. Peng, X. Peng, and M. Pecht, "Lithium-ion battery remaining useful life estimation based on nonlinear ar model combined with degradation feature," in *Proc. Annu. Conf. Prognostics Health Manage. Soc.*, vol. 3, 2012, pp. 1803–1836.
[32] D. Liu, Y. Luo, J. Liu, Y. Peng, L. Guo, and M. Pecht, "Lithium-ion battery remaining useful life estimation based on fusion nonlinear degradation AR model and RPF algorithm," *Neural Comput. Appl.*, vol. 25, nos. 3–4, pp. 557–572, Sep. 2014.
[33] Z. Xia and J. A. A. Qahouq, "Adaptive and fast state of health estimation method for lithium-ion batteries using online complex impedance and artificial neural network," in *Proc. IEEE Appl. Power Electron. Conf. Expo. (APEC)*, Mar. 2019, pp. 3361–3365.
[34] S. Zhang, B. Zhai, X. Guo, K. Wang, N. Peng, and X. Zhang, "Synchronous estimation of state of health and remaining useful lifetime for lithium-ion battery using the incremental capacity and artificial neural networks," *J. Energy Storage*, vol. 26, Dec. 2019, Art. no. 100951.
[35] H. Pan, Z. Lü, H. Wang, H. Wei, and L. Chen, "Novel battery state-of-health online estimation method using multiple health indicators and an extreme learning machine," *Energy*, vol. 160, pp. 466–477, Oct. 2018.
[36] S. Shen, M. Sadoughi, X. Chen, M. Hong, and C. Hu, "A deep learning method for online capacity estimation of lithium-ion batteries," *J. Energy Storage*, vol. 25, Oct. 2019, Art. no. 100817.
[37] A. Eddahech, O. Briat, N. Bertrand, J.-Y. Delétage, and J.-M. Vinassa, "Behavior and state-of-health monitoring of Li-ion batteries using impedance spectroscopy and recurrent neural networks," *Int. J. Elect. Power Energy Syst.*, vol. 42, no. 1, pp. 487–494, Nov. 2012.
[38] Y. Zhang, R. Xiong, H. He, and M. G. Pecht, "Long short-term memory recurrent neural network for remaining useful life prediction of lithium-ion batteries," *IEEE Trans. Veh. Technol.*, vol. 67, no. 7, pp. 5695–5705, Jul. 2018.
[39] T. Qin, S. Zeng, and J. Guo, "Robust prognostics for state of health estimation of lithium-ion batteries based on an improved PSO-SVR model," *Microelectron. Rel.*, vol. 55, nos. 9–10, pp. 1280–1284, Aug./Sep. 2015.
[40] T. Tao and W. Zhao, "A support vector regression-based prognostic method for Li-ion batteries working in variable operating states," in *Proc. Prognostics Syst. Health Manage. Conf. (PHM-Chengdu)*, Oct. 2016, pp. 1–5.
[41] A. Widodo, M.-C. Shim, W. Caesarendra, and B.-S. Yang, "Intelligent prognostics for battery health monitoring based on sample entropy," *Expert Syst. Appl.*, vol. 38, no. 9, pp. 11763–11769, Sep. 2011.
[42] Y. Zhou, M. Huang, Y. Chen, and Y. Tao, "A novel health indicator for on-line lithium-ion batteries remaining useful life prediction," *J. Power Sources*, vol. 321, pp. 1–10, Jul. 2016.
[43] Z. Wang, J. Ma, and L. Zhang, "State-of-health estimation for lithium-ion batteries based on the multi-Island genetic algorithm and the Gaussian process regression," *IEEE Access*, vol. 5, pp. 21286–21295, 2017.
[44] F.-K. Wang and T. Mamo, "Gradient boosted regression model for the degradation analysis of prismatic cells," *Comput. Ind. Eng.*, vol. 144, Jun. 2020, Art. no. 106494.
[45] F. Yang, D. Wang, F. Xu, Z. Huang, and K.-L. Tsui, "Lifespan prediction of lithium-ion batteries based on various extracted features and gradient boosting regression tree model," *J. Power Sources*, vol. 476, Nov. 2020, Art. no. 228654.
[46] D. Liu, W. Xie, H. Liao, and Y. Peng, "An integrated probabilistic approach to lithium-ion battery remaining useful life estimation," *IEEE Trans. Instrum. Meas.*, vol. 64, no. 3, pp. 660–670, Mar. 2015.
[47] I.-S. Han and C.-B. Chung, "Performance prediction and analysis of a PEM fuel cell operating on pure oxygen using data-driven models: A comparison of artificial neural network and support vector machine," *Int. J. Hydrogen Energy*, vol. 41, no. 24, pp. 10202–10211, Jun. 2016.
[48] M. Kirk, *Thoughtful Machine Learning: Test-Driven Approach HSKIP 1emplus EM Minus EM Relax*. Sebastopol, CA, USA: O'Reilly Media, 2014.
[49] S. A. Kalogirou, "Artificial neural networks in renewable energy systems applications: A review," *Renew. Sustain. Energy Rev.*, vol. 5, no. 4, pp. 373–401, Dec. 2001.
[50] G.-B. Huang, Q.-Y. Zhu, and C.-K. Siew, "Extreme learning machine: Theory and applications," *Neurocomputing*, vol. 70, nos. 1–3, pp. 489–501, 2006.

[51] J. Tian, R. Xiong, W. Shen, and F. Sun, "Electrode ageing estimation and open circuit voltage reconstruction for lithium ion batteries," *Energy Storage Mater.*, vol. 37, pp. 283–295, May 2021.
[52] T. Tieleman and G. Hinton, "Lecture 6.5-RMSPROP: Divide the gradient by a running average of its recent magnitude," *COURSERA, Neural Netw. Mach. Learn.*, vol. 4, no. 2, pp. 26–31, 2012.
[53] N. Srivastava, G. Hinton, A. Krizhevsky, I. Sutskever, and R. Salakhutdinov, "Dropout: A simple way to prevent neural networks from overfitting," *J. Mach. Learn. Res.*, vol. 15, no. 1, pp. 1929–1958, 2014.
[54] Y. Xing, E. W. M. Ma, K.-L. Tsui, and M. Pecht, "An ensemble model for predicting the remaining useful performance of lithium-ion batteries," *Microelectron. Rel.*, vol. 53, pp. 811–820, Jun. 2013.
[55] Z. Liu, G. Sun, S. Bu, J. Han, X. Tang, and M. Pecht, "Particle learning framework for estimating the remaining useful life of lithium-ion batteries," *IEEE Trans. Instrum. Meas.*, vol. 66, no. 2, pp. 280–293, Feb. 2017.
[56] W. He, N. Williard, M. Osterman, and M. Pecht, "Prognostics of lithium-ion batteries based on Dempster–Shafer theory and the Bayesian Monte Carlo method," *J. Power Sources*, vol. 196, pp. 10314–10321, Dec. 2011.
[57] C. Lyu, Q. Lai, T. Ge, H. Yu, L. Wang, and N. Ma, "A lead-acid battery's remaining useful life prediction by using electrochemical model in the particle filtering framework," *Energy*, vol. 120, pp. 975–984, Feb. 2017.
[58] W.-A. Yang, M. Xiao, W. Zhou, Y. Guo, and W. Liao, "A hybrid prognostic approach for remaining useful life prediction of lithium-ion batteries," *Shock Vib.*, vol. 2016, pp. 1–15, Jan. 2016.
[59] J. Kennedy and R. C. Eberhart, "A discrete binary version of the particle swarm algorithm," in *Proc. IEEE Int. Conf. Syst., Man, Cybern. Comput. Simulation*, vol. 5, Oct. 1997, pp. 4104–4108.
[60] J. Kennedy and R. Eberhart, "Particle swarm optimization," in *Proc. Int. Conf. Neural Netw. (ICNN)*, vol. 4, Nov./Dec. 1995, pp. 1942–1948.
[61] Y. Song and P. Liò, "A new approach for epileptic seizure detection: Sample entropy based feature extraction and extreme learning machine," *J. Biomed. Sci. Eng.*, vol. 3, no. 6, p. 556, 2010.
[62] B. Saha and K. Goebel, "Battery data set," NASA AMES Prognostics Data Repository, 2007.
[63] Y. Wu, Q. Xue, J. Shen, Z. Lei, Z. Chen, and Y. Liu, "State of health estimation for lithium-ion batteries based on healthy features and long short-term memory," *IEEE Access*, vol. 8, pp. 28533–28547, 2020.
[64] H. Tian, P. Qin, K. Li, and Z. Zhao, "A review of the state of health for lithium-ion batteries: Research status and suggestions," *J. Cleaner Prod.*, vol. 261, Jul. 2020, Art. no. 120813.
[65] S. Shen, B. Liu, K. Zhang, and S. Ci, "Toward fast and accurate SOH prediction for lithium-ion batteries," *IEEE Trans. Energy Convers.*, vol. 36, no. 3, pp. 2036–2046, Sep. 2021.
[66] O. R. Shishvan, D.-S. Zois, and T. Soyata, "Machine intelligence in healthcare and medical cyber physical systems: A survey," *IEEE Access*, vol. 6, pp. 46419–46494, 2018.
[67] B. Neal, S. Mittal, A. Baratin, V. Tantia, M. Scicluna, S. Lacoste-Julien, and I. Mitliagkas, "A modern take on the bias-variance tradeoff in neural networks," 2018, *arXiv:1810.08591*. [Online]. Available: http://arxiv.org/abs/1810.08591
[68] M. Lucu, E. Martinez-Laserna, I. Gandiaga, and H. Camblong, "A critical review on self-adaptive Li-ion battery ageing models," *J. Power Sources*, vol. 401, pp. 85–101, Oct. 2018.
[69] O. Giustolisi, "Sparse solution in training artificial neural networks," *Neurocomputing*, vol. 56, pp. 285–304, Jan. 2004.
[70] M. Nasiri, B. Minaei, and Z. Sharifi, "Adjusting data sparsity problem using linear algebra and machine learning algorithm," *Appl. Soft Comput.*, vol. 61, pp. 1153–1159, Dec. 2017.

TSUYOSHI OJI received the B.E. degree in electrical engineering and automation from Tsinghua University, Beijing, China, in 2019. He is currently pursuing the M.S. degree in environment science and new energy technology with Tsinghua-Berkeley Shenzhen Institute, Tsinghua University. His research interests include state and parameter estimation and data-driven prognostics of lithium ion battery.

YANGLIN ZHOU (Student Member, IEEE) received the Ph.D. degree from the University of Chinese Academy of Sciences. He is currently a Postdoctoral Researcher with the Department of Electrical and Engineering, Tsinghua University, China. His research interests include data analysis and algorithm design, demand response in smart grid, P2P energy sharing in energy internet, and green computing in 5G.

SONG CI (Senior Member, IEEE) is currently a Professor with the Department of Electrical Engineering, Tsinghua University. His research has been supported by NSFC and other funding sources. His current research interests include large-scale dynamic complex system modeling and optimization, energy internet, digital battery energy storage, and green computing and communications. He has authored more than 200 peer-reviewed articles in his research areas. He is a member of ACM and AAAS. He has served as an Editor or a Guest Editor for many journals, such as the IEEE TRANSACTIONS ON CIRCUITS AND SYSTEMS FOR VIDEO TECHNOLOGY, the IEEE JOURNAL ON SELECTED AREAS IN COMMUNICATIONS, IEEE ACCESS, and the IEEE WIRELESS NETWORKS.

FEIYU KANG received the B.S. and M.S. degrees in mechanical engineering from Tsinghua University, Beijing, China, in 1986 and 1988, respectively, and the Ph.D. degree in mechanical engineering from The Hong Kong University of Science and Technology, Hong Kong, in 1997. He is currently a Professor with the School of Materials Science and Engineering, Tsinghua University. His current research interests include nano-carbon materials, graphite and its intercalation compounds, lithium ion battery and super-capacitors, and new type batteries, such as zinc ion battery and fuel cell.

XI CHEN received the master's degree from Beihang University, Beijing, China, in 2016. She is currently an Engineer with Beijing Electric Power Research Institute, Beijing. Her current research interests include testing technology of electric vehicles supply equipment and testing of EES system in electric charging stations.

XIULAN LIU (Member, IEEE) received the master's degree from Sichuan University, Chengdu, China, in 2009. Since August 2009, she has been an Engineer with Beijing Electric Power Research Institute, Beijing, China. Her current research interests include test technology of electric vehicles supply equipment, battery management systems, and wireless power transfer.